

1 **Tropopause Evolution in a Rapidly Intensifying Tropical Cyclone: A Static**
2 **Stability Budget Analysis**

3 Patrick Duran* and John Molinari

4 *University at Albany, State University of New York, Albany, NY*

5 **Corresponding author address:* Department of Atmospheric and Environmental Sciences, Univer-
6 sity at Albany, State University of New York, 1400 Washington Avenue, Albany, NY.

7 E-mail: pduran2008@gmail.com

ABSTRACT

8 Enter the text of your abstract here.

9 **1. Introduction**

10 **2. Model Setup**

11 Put description of Fig. 1 in this section. Don't forget to mention 1-2-1 smoother.

12 **3. Budget Computation**

13 **4. Results**

14 *a. Static stability evolution*

15 The simulated static stability evolution closely follows that observed in Hurricane Patricia (2015;
16 Duran and Molinari 2018). The average N^2 over the first day of the simulation (Fig. 2a) indi-
17 cates the presence of a static stability maximum about 400 m above the cold-point tropopause.
18 This lower-stratospheric stable layer had begun to erode during the initial spin-up period, with
19 the maximum destabilization occurring at the innermost radii. This decrease in static stability
20 continued into the second day of the simulation (Fig. 2b) as the storm intensified to hurricane
21 strength (Fig. 1). Destabilization was particularly pronounced over the developing eye, where the
22 time-mean cold-point tropopause height increased by up to 400 m compared to the previous day.
23 Over the developing eyewall and outer rainband regions, meanwhile, the time-mean tropopause
24 height remained nearly constant. During the third day of the simulation (Fig. 2c), static stability
25 over the eye region continued to decrease, and the cold-point tropopause height rose to 18.3 km
26 at the storm center. The tropopause sloped sharply downward over the innermost radii, reaching
27 the 16.4-km level near the 50-km radius. This local minimum in tropopause height corresponded
28 to the eyewall region, where upper-tropospheric static stability increased during this time period.
29 Outside of the eyewall region, static stability began to increase in the layer immediately overly-

ing the cold-point tropopause. This stable layer sloped upward with radius, which corresponded to an upward-sloping tropopause radially outside of the eyewall region. Over the next 24 hours (Fig. 2d), as the storm’s maximum 10-m wind speed leveled off near 80 m s^{-1} (Fig. 1), the upper-tropospheric static stability within the eyewall region continued to strengthen, along with the static stability within the lower stratosphere radially outside of the eyewall. As the stable layer strengthened, its altitude rose slightly, which corresponded to a slight increase in tropopause height outside of the eyewall during this period. Within the upper troposphere radially outside of the eyewall, meanwhile, static stability decreased such that it was nearly neutral in a thin layer between the 120- and 150-km radii. The eye region likewise continued to destabilize, and the cold-point tropopause height increased to a level above 18.5 km.

b. Potential temperature budget analysis

The left column of Fig. 4 depicts 24-hour changes in N^2 over each of the four days of the simulation. These represent bulk changes computed by subtracting the instantaneous N^2 at the initial time from the instantaneous N^2 at the final time. The middle column of Fig. 4 represents the change in N^2 computed using Eq. XXX and the process described in Section 3. The residual between these two computations (Fig. 4, right column) is much smaller than the change in N^2 , meaning that the budget performs well within the analysis domain.

Acknowledgments. Start acknowledgments here.

References

Duran, P., and J. Molinari, 2018: Dramatic tropopause variability during the rapid intensification of hurricane patricia (2015). *Mon. Wea. Rev.*, **XXX (X)**, XXX–XXX.

51 LIST OF FIGURES

- 52 **Fig. 1.** The maximum 10-m wind speed (top panel; m s^{-2}) and minimum sea-level pressure (bottom
53 panel; hPa) in the simulated storm (blue lines) and from Hurricane Patricia's best track (red
54 stars). 6
- 55 **Fig. 2.** Twenty-four-hour averages of squared Brunt-Väisälä frequency (10^{-4} s^{-2}) over the first four
56 days of the simulation. Orange lines represent the cold-point tropopause computed from the
57 mean temperature field over the same time periods. 7
- 58 **Fig. 3.** Left panels: Twenty-four-hour changes in squared Brunt-Väisälä frequency (10^{-4} s^{-2}) over
59 (a) 0-24 hours, (b) 24-48 hours, (c) 48-72 hours, (d) 72-96 hours. Middle Panels: The N^2
60 change over the same time periods computed using Eq. XXX. Right Panels: The budget
61 residual over the same time periods, computed by subtracting the budget change (middle
62 column) from the model change (left column). 8
- 63 **Fig. 4.** Time series of the contribution of each of the budget terms to the squared Brunt-Väisälä
64 frequency (10^{-4} s^{-2}) tendency. For each budget term, the absolute value of the N^2 tendency
65 is averaged both spatially and temporally over 1-hour periods and within the radius-height
66 domain depicted in Figs. 2 and 3. 9

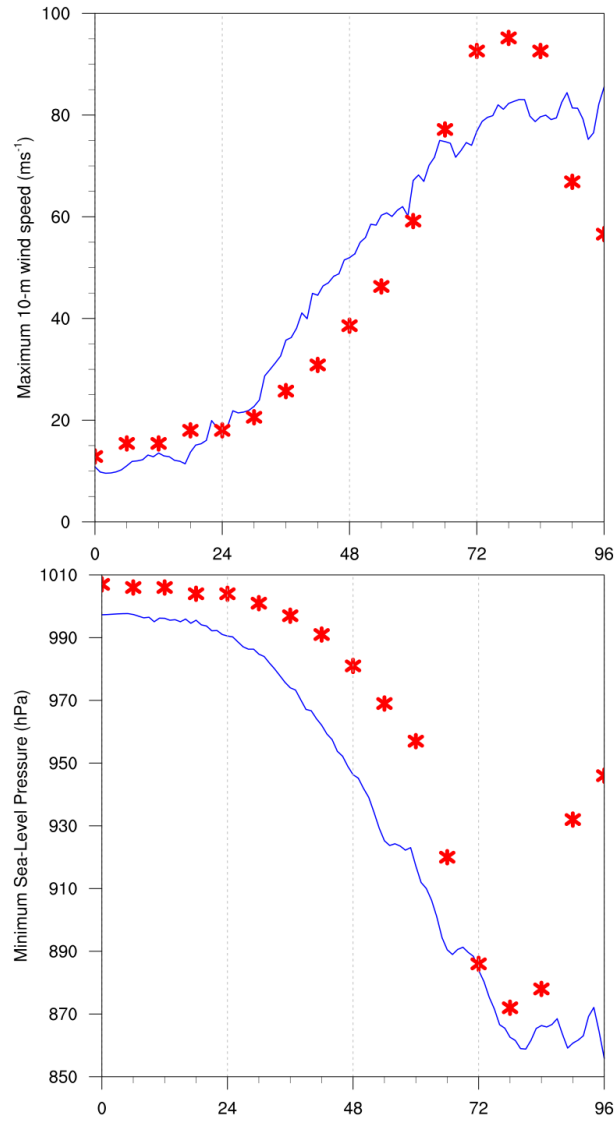


FIG. 1. The maximum 10-m wind speed (top panel; m s^{-2}) and minimum sea-level pressure (bottom panel; hPa) in the simulated storm (blue lines) and from Hurricane Patricia's best track (red stars).

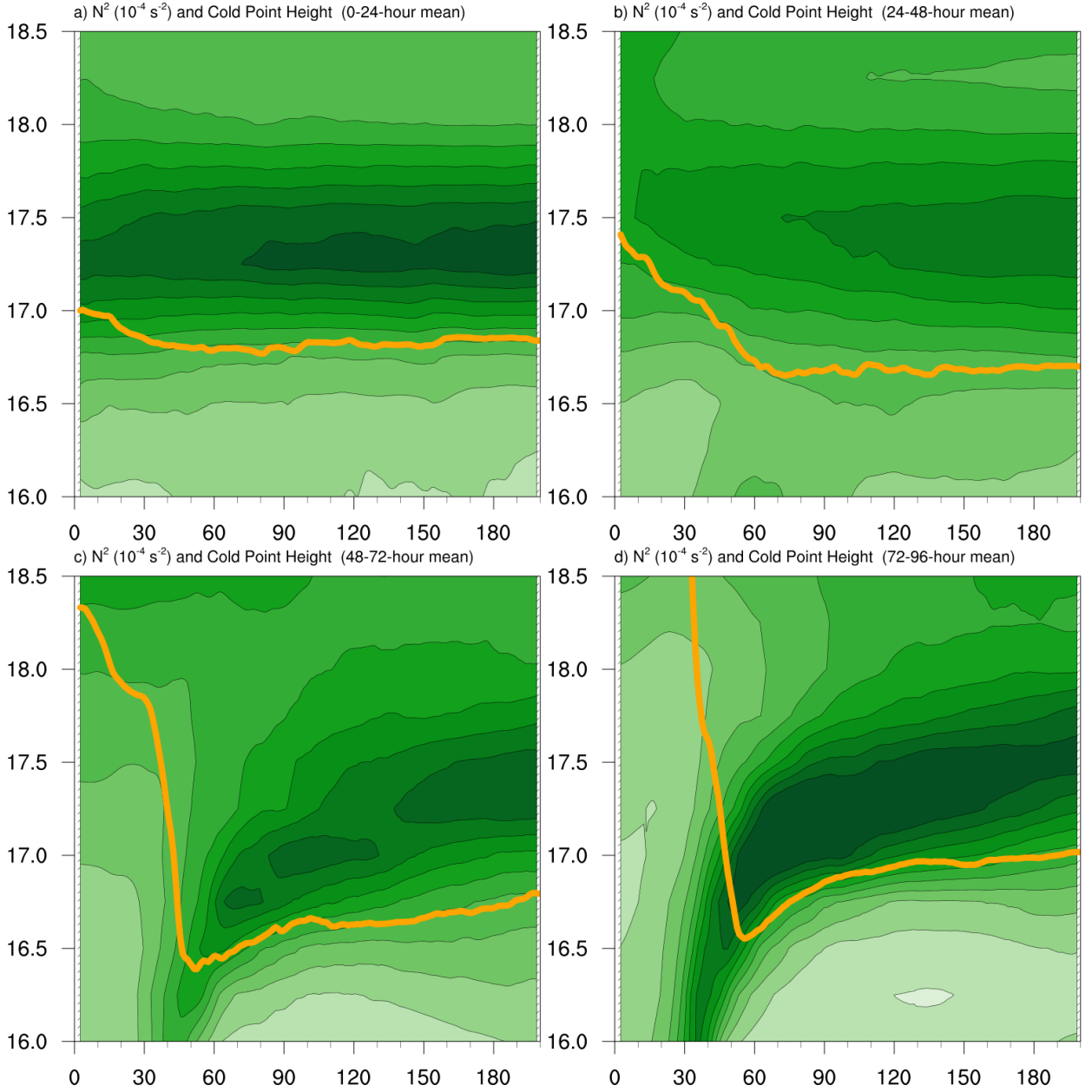
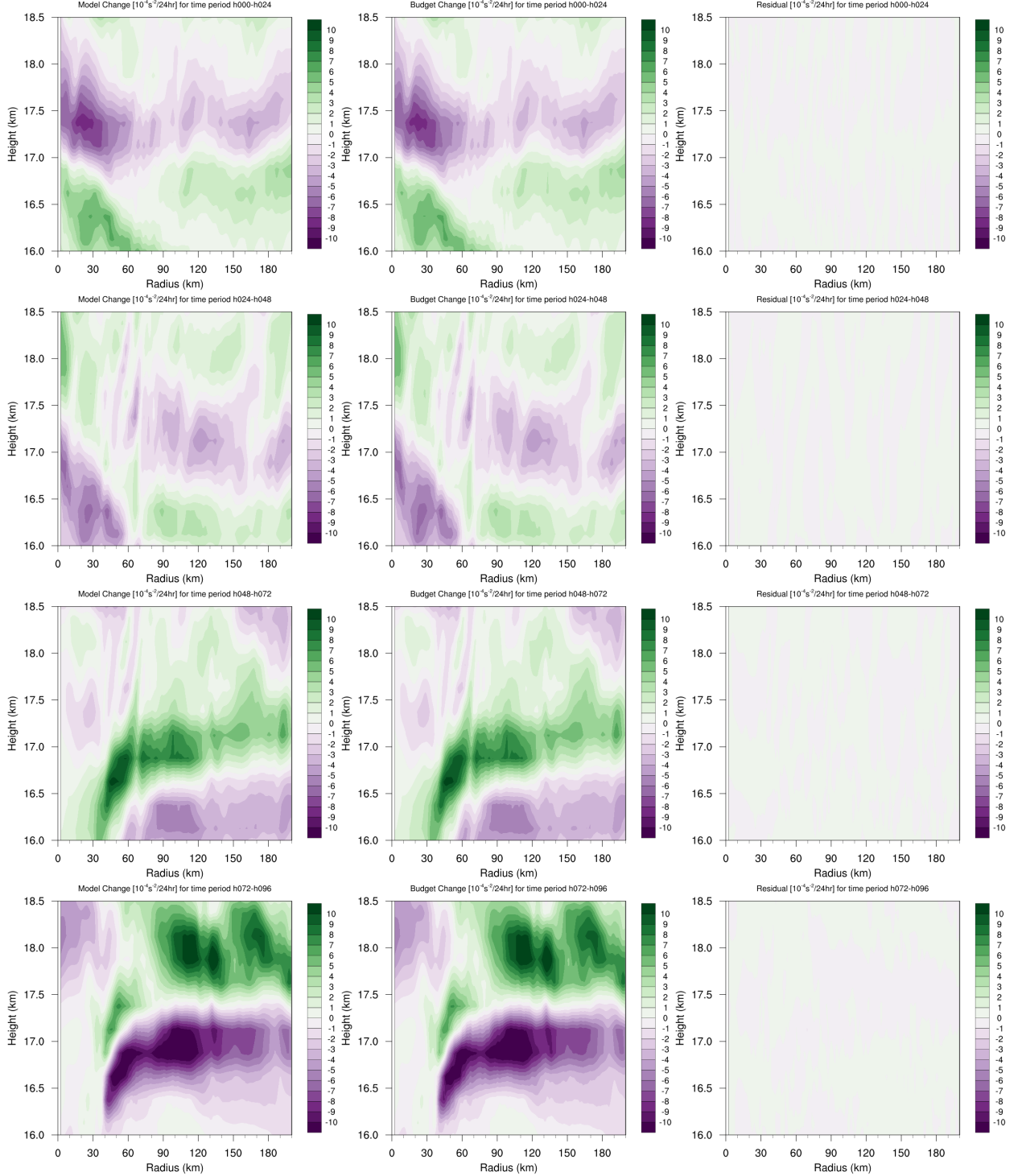


FIG. 2. Twenty-four-hour averages of squared Brunt-Väisälä frequency (10^{-4} s^{-2}) over the first four days of the simulation. Orange lines represent the cold-point tropopause computed from the mean temperature field over the same time periods.



72 FIG. 3. Left panels: Twenty-four-hour changes in squared Brunt-Väisälä frequency (10^{-4} s^{-2}) over (a) 0-24
 73 hours, (b) 24-48 hours, (c) 48-72 hours, (d) 72-96 hours. Middle Panels: The N^2 change over the same time
 74 periods computed using Eq. XXX. Right Panels: The budget residual over the same time periods, computed by
 75 subtracting the budget change (middle column) from the model change (left column).

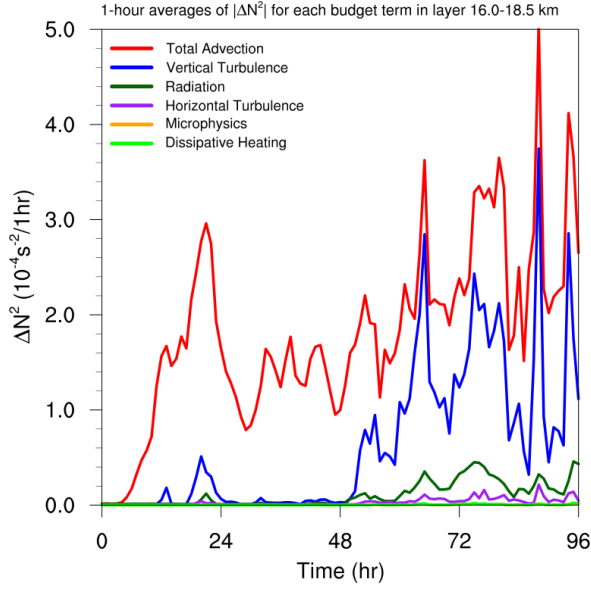


FIG. 4. Time series of the contribution of each of the budget terms to the squared Brunt-Väisälä frequency
 (10^{-4} s^{-2}) tendency. For each budget term, the absolute value of the N^2 tendency is averaged both temporally and
 spatially over 1-hour periods, using output every minute, and within the radius-height domain depicted in Fig. 4.